Acta Pharmacologica Sinica

ARTICLE

Stratifin promotes renal dysfunction in ischemic and nephrotoxic AKI mouse models via enhancing RIPK3-mediated necroptosis

Fang Wang[1], Jia-nan Wang[1], Xiao-yan He[1], Xiao-guo Suo[1], Chao Li[1], Wei-jian Ni[1,2], Yu-ting Cai[1], Yuan He[1], Xin-yun Fang[1], Yu-hang Dong[1], Tian Xing[3], Ya-ru Yang[1], Feng Zhang[4], Xiang Zhong[5], Hong-mei Zang[1], Ming-ming Liu[1], Jun Li[1], Xiao-ming Meng[1] and Juan Jin[6]

Stratifin (SFN) is a member of the 14-3-3 family of highly conserved soluble acidic proteins, which regulates a variety of cellular activities such as cell cycle, cell growth and development, cell survival and death, and gene transcription. Acute kidney injury (AKI) is prevalent disorder characterized by inflammatory response, oxidative stress, and programmed cell death in renal tubular epithelial cells, but there is still a lack of effective therapeutic target for AKI. In this study, we investigated the role of SFN in AKI and the underlying mechanisms. We established ischemic and nephrotoxic AKI mouse models caused by ischemia–reperfusion (I/R) and cisplatin, respectively. We conducted proteomic and immunohistochemical analyses and found that SFN expression levels were significantly increased in AKI patients, cisplatin- or I/R-induced AKI mice. In cisplatin- or hypoxia/reoxygenation (H/R)-treated human proximal tubule epithelial cells (HK2), we showed that knockdown of SFN significantly reduced the expression of kidney injury marker Kim-1, attenuated programmed cell death and inflammatory response. Knockdown of SFN also significantly alleviated the decline of renal function and histological damage in cisplatin-caused AKI mice in vivo. We further revealed that SFN bound to RIPK3, a key signaling modulator in necroptosis, to induce necroptosis and the subsequent inflammation in cisplatin- or H/R-treated HK2 cells. Overexpression of SFN increased Kim-1 protein levels in cisplatin-treated MTEC cells, which was suppressed by RIPK3 knockout. Taken together, our results demonstrate that SFN that enhances cisplatin- or I/R-caused programmed cell death and inflammation via interacting with RIPK3 may serve as a promising therapeutic target for AKI treatment.

Keywords: acute kidney injury; programmed cell death; necroptosis; stratifin; RIPK3

Acta Pharmacologica Sinica (2022) 43:330–341; https://doi.org/10.1038/s41401-021-00649-w

INTRODUCTION

Acute kidney injury (AKI) is a clinical syndrome characterized by acute renal dysfunction [1], and in recent years, both the incidence and mortality rate of this condition have been increasing [2, 3]. Although the pathogenesis of AKI has been well-documented, there are currently no effective treatments or preventive measures [4–6]. The main causes of AKI are ischemia, hypoxia [7, 8], sepsis [9], and nephrotoxic drugs (ex. cisplatin) [10–12]. Emerging evidence indicates that there are several pathological mechanisms of AKI, including tubule necroptosis and inflammation [13, 14], and although these processes have been verified to play essential roles in AKI, potential mechanisms and effective treatments are still lacking.

Stratifin (SFN) is a highly conserved soluble acidic protein in the 14-3-3 family that can spontaneously self-assemble into dimers [15, 16]. This family consists of seven isoforms denoted β, ε, γ, η, τ, ζ, and δ; 14-3-3 proteins are crucial for a wide range of cellular activities, including cell proliferation, protein trafficking, DNA replication, apoptosis, and cell survival [17, 18]. Using isobaric tags for relative and absolute quantitation (iTRAQ), we found that SFN (14-3-3δ) was highly expressed in ischemia–reperfusion (I/R) mice, which is consistent with the findings of a previous study [15, 16]. SFN has been shown to aid in modulating the inflammatory response in multiple disorders, including autoimmune and respiratory diseases [19, 20]. SFN is also involved in the regulation of cell proliferation, differentiation, and death in immune system diseases and tumors [19, 21, 22], and these findings suggest that its role in cell death and inflammation is critical. It is generally acknowledged that the regulation of inflammation and programmed cell death is a central process in the maintenance of

[1]Inflammation and Immune Mediated Diseases Laboratory of Anhui Province, Anhui Institute of Innovative Drugs, School of Pharmacy, Anhui Medical University, The Key Laboratory of Anti-inflammatory of Immune Medicines, Ministry of Education, Hefei 230032, China; [2]Department of Pharmacy, Anhui Provincial Hospital, The First Affiliated Hospital of USTC, Division of Life Sciences and Medicine, University of Science and Technology of China, Hefei 230001, China; [3]Hospital of Stomatology, Anhui Medical University, Key Laboratory of Oral Diseases Research of Anhui Province, Hefei 230032, China; [4]Department of Pharmacy, Changzheng Hospital, Naval Medical University, Shanghai 200003, China; [5]Department of Nephrology, Sichuan Academy of Medical Sciences & Sichuan Provincial People's Hospital, School of Medicine, University of Electronic Science and Technology of China, Chengdu 610072, China and [6]School of Basic Medical Sciences, Anhui Medical University, Hefei 230032, China
Correspondence: Xiao-ming Meng (mengxiaoming@ahmu.edu.cn) or Juan Jin (jinjuan@ahmu.edu.cn)
These authors contributed equally: Fang Wang, Jia-nan Wang, Xiao-yan He

Received: 24 November 2020 Accepted: 12 March 2021
Published online: 8 April 2021

renal homeostasis [23–25]; therefore, we hypothesized that SFN regulates renal function, programmed death of tubular cells, and the inflammatory response in AKI.

To verify this hypothesis, we studied the expression and function of SFN in models of cisplatin- and hypoxia–reoxygenation (H/R)-induced cell damage using renal tubular cells in vitro and a model of cisplatin-induced nephropathy treated with lentivirus-packaged SFN shRNA in vivo.

MATERIALS AND METHODS

Reagents and materials

Cisplatin was obtained from Sigma-Aldrich (St. Louis, MO, USA). Fetal bovine serum (FBS), DMEM, and other cell culture reagents were purchased from Invitrogen (Carlsbad, CA, USA). The antibody-related information is as follows. The anti-SFN antibody (ab14123) was obtained from Abcam (Shanghai, China; WB: 1:1000, IP: 1:500, IF: 1:500, IHC: 1:500). The anti-p-MLKL antibody (#91689) was obtained from Cell Signaling Technology (CST, Danvers, MA, USA; IF: 1:200). The anti-TNF-α antibody (bs-2081R) was obtained from BiossBiotechnology (Bioss, Beijing, China; IHC: 1:200). The anti-β-Actin antibody (bsm-33036M) was obtained from BiossBiotechnology (Bioss, Beijing, China; WB: 1:800). The anti-Kim-1 antibody (bs-2713R) was also obtained from BiossBiotechnology (Bioss, Beijing, China; WB: 1:800, IF: 1:500, IHC: 1:200). The anti-RIPK3 (sc-135170) and anti-RIPK1 (sc-7881) antibodies were obtained from Santa Cruz Biotechnology (CA, USA; WB: 1:800, IP: 1:500). The anti-F4/80 (sc-26643-R) antibody was also obtained from Santa Cruz Biotechnology (CA, USA; IHC: 1:200). Lipofectamine 2000 was purchased from SciencBio Technology (Invitrogen, Carlsbad, CA, USA). The Protein Assay Kit was purchased from Beyotime Institute of Biotechnology (Jiangsu, China). Periodic acid-Schiff (PAS), creatinine (Cr), and blood urea nitrogen (BUN) assay kits were obtained from Nanjing Jiancheng Bioengineering Institute (Nanjing, China).

Establishment of the AKI mouse model

Male C57BL/6 mice (6–8 weeks of age, 20–25 g) were obtained from Jinan Pengyue Experimental Animal Breeding Company. All animal procedures were approved by the Animal Experimentation Ethics Committee of Anhui Medical University, Anhui, China. To test the effect of SFN on cisplatin-induced AKI, adult male mice were randomly divided into the following groups ($n = 6$–8 per group): control, cisplatin, SFN knockdown, and cisplatin + SFN knockdown. Except for those in the control group, all animals were intraperitoneally injected with a single dose of cisplatin at 20 mg/kg to induce AKI, and after 72 h of cisplatin treatment, mice in all groups were sacrificed. To establish I/R-induced AKI, renal I/R was induced in mice as previously described [26]. Briefly, mice were subjected to I/R by bilateral clamping for 40 min followed by reperfusion [27, 28]. Kidney tissue samples were harvested for PAS staining, immunohistochemistry, Western blotting, and real-time PCR as reported previously, and blood samples were collected for BUN and Cr measurement in accordance with the manufacturer's instructions.

Lentivirus-mediated SFN knockdown in mice

Mouse SFN shRNA was obtained from GenePharm (Shanghai, China). The vector used for shRNA delivery was the LV3 vector, and the target sequence of the shRNA was 5′-CCGAACGCTATGAG GACAT-3′. To silence SFN expression, the lentiviral vector was injected into mice through the tail vein, and according to the manufacturer's instructions, the cisplatin-induced mouse model was established after 96 h of lentiviral expression for further analysis.

Isobaric tags for relative and absolute quantitation (iTRAQ)

Total protein was extracted from mice in the normal and I/R groups using the cold acetone method, and protein quality was examined by SDS-PAGE. A BCA assay was then used to determine the protein concentration in the supernatant. For each sample, proteins were first precipitated with ice-cold acetone and were then digested with sequencing-grade modified trypsin (Promega, Madison, WI, USA) at 37 °C overnight. Next, the labeled samples were combined and dried in a vacuum. Finally, strong cation exchange (SCX) fractionation and liquid chromatography–tandem mass spectrometry analyses were carried out.

Knockdown and overexpression (OE) of SFN in tubular epithelial cells

SFN was knocked down by transfection of siRNA sequences obtained from GenePharm (Shanghai, China), and the siRNA sequence was 5′-CCGAACGCUAUGAGGACAUTTAUGUCCUCAUAG CGUUCGGTT-3′. The SFN OE plasmid was obtained from Hanbio Biotechnology Co., Ltd. (Shanghai, China), and the plasmid used for SFN OE was pcDNA3.1-EF1a-mcs-3flag-CMV-GFP. Briefly, cells were seeded in six-well plates and transfected with SFN siRNA/SFN OE plasmid or the corresponding control constructs using Lipo2000 transfection reagent (Invitrogen, Carlsbad, CA, USA). Cells were incubated with Opti-MEM at 37 °C and 5% CO_2 for 6 h. Cells were cultured in DMEM containing 5% FBS. Two kinds of cell damage models using renal tubular cells in vitro were established. The relationship between SFN and AKI was analyzed by Western blotting, real-time PCR, and immunofluorescence.

CRISPR-Cas9-based RIPK3 knockout

Lentiviral vectors containing a pair of gRNAs targeting exon 3 of mouse RIPK3 and CRISPR-associated protein 9 (Cas9; lenti Cas9-GFP) were obtained from Shanghai Genechem. Mouse renal tubule epithelial cells (MTECs) were infected with GFP lentivirus and sorted by green fluorescent protein (GFP) expression. Single GFP-labeled MTECs were plated in 96-well plates using a flow cytometer and grown for 7–10 days. The isolated single clones were subjected to PCR and DNA sequencing for knockout validation. The target sequence of the sgRNA was 5′-GCAGAATGT TAGAGGGCTTG-3′.

Cell culture

The human proximal tubule epithelial cell line (HK2) and MTECs were obtained from the American Type Culture Collection (ATCC, Manassas, VA, USA). HK2 cells were routinely cultured in DMEM-F12 supplemented with 5% FBS. Cells were starved for 12 h with 0.5% FBS and were then treated with cisplatin (20 μM) for 24 h. Hypoxia (0.1% O_2) was induced in 0.5% low-glucose medium for 12 h prior to reoxygenation in normal medium for 6 h for Western blot analysis or reoxygenation for 3 h for real-time PCR analysis. Cells were harvested and analyzed by real-time PCR and Western blotting for indications of tubular injury, inflammation, and necroptosis.

Human samples

All human kidney samples were obtained from the First Affiliated Hospital of Anhui Medical University (Hefei, China). Normal kidney tissue was sampled from paracancerous tissue of three patients (without injury) with renal cancer. AKI renal tissues were obtained from puncture tissue of three patients with AKI. The clinical features of the patients with AKI are listed in Table S1. The study protocols concerning human subjects were consistent with the principles of the Declaration of Helsinki and were approved by the Biomedical Ethics Committee of Anhui Medical University.

Renal RNA extraction and real-time PCR

Total RNA was obtained from fresh kidney homogenate or cultured HK2 cells with RNA-iso reagent (Qiagen, Valencia, CA). A NanoDrop 2000 spectrophotometer (Thermo Scientific, USA) was used to quantify the RNA concentration. Total RNA was reverse transcribed into cDNA according to the manufacturer's instructions using a Bio-Rad kit. The real-time PCR mixture contained 0.3 μL each of the forward and reverse primers for each gene, 5 μL of Bio-Rad iQ

Table 1. Primer sequences used in real-time PCR.

Genes	Forward primer (5′–3′)	Reverse primer (5′–3′)
(A) Mouse		
TNF-α	CATCTTCTCAAAATTCGAGTGACAA	TGGGAGTAGACAAGGTACAACCC
IL-6	GAGGATACCACTCCCAACAGACC	AAGTGCATCATCGTTGTTCATACA
IL-1β	CTTTGAAGTTGACGGACCC	TGAGTGATACTGCCTGCCTG
Kim-1	CAGGGAAGCCGCAGAAAA	GAGACACGGAAGGCAACCAC
SFN	GGAGAGAGCCAGTCTGATCC	GCTGCCATGTCTTCATACCG
β-actin	CATTGCTGACAGGATGCAGAA	ATGGTGCTAGGAGCCAGAGC
(B) Human		
TNF-α	CATCTTCTCAAAATTCGAGTGACAA	TGGGAGTAGACAAGGTACAACCC
IL-6	CGGGAACGAAAGAGAAGCTCTA	GAGCAGCCCCAGGGAGAA
IL-1β	CAACCAACAAGTGATATTCTCCATG	GATCCACACTCTCCAGCTGCA
Mcp-1	GCTGAGACTAACCCAGAAACATC	GAATGAAGGTGGCTGCTATGA
Kim-1	CTGCAGGGAGCAATAAGGAG	TCCAAAGGCCATCTGAAGAC
SFN	CCTTGTGGCTGAGAACTGG	AGACATGCTTTCCCTCAATCT
β-actin	CGCCGCCAGCTCACCATG	CACGATGGAGGGGAAGAC

SYBR-Green Supermix with Opticon 2 (Bio-Rad, USA), 2.4 μL of enzyme-free water, and 2 μL of cDNA solution. The levels of SFN, Kim-1, IL-1β, IL-6, TNF-α, Mcp-1, and β-actin were determined by real-time PCR with SYBR-Green I in a CFX96 real-time PCR detection system (Bio-Rad, USA). The ratio for the mRNA of interest was normalized to that of β-actin and presented as the mean ± SEM value. The real-time PCR thermal cycling conditions were as follows: denaturation at 95 °C for 20 s, annealing at 58 °C for 20 s, elongation at 72 °C for 20 s, and amplification for 40 cycles for each primer pair. β-Actin was used for normalization of the relative mRNA ratios of the other genes [26]. The primer sequences are listed in Table 1 [13].

Western blot analysis

Proteins from the renal cortex and cultured cells were extracted with RIPA buffer (Beyotime, Jiangsu, China) containing PMSF. A BCA kit (Beyotime, Jiangsu, China) was used to measure protein concentrations. Western blotting was performed as described previously [29, 30]. Membranes were incubated with 5% milk in PBS for 1.5 h to block nonspecific binding and were then incubated with appropriate antibodies, i.e., rabbit anti-Kim-1, rabbit anti-RIPK3, mouse anti-SFN, and mouse anti-β-actin overnight at 4 °C. Membranes were incubated with an IRDye 800-conjugated secondary antibody for 1.5 h at room temperature (Rockland Immunochemicals, USA). Images were acquired with a LiCor/Odyssey infrared imaging system (LI-COR Biosciences, Lincoln, NE, USA). Densitometric analysis was performed by measuring the intensities of the bands using ImageJ software (NIH, Bethesda, MD, USA).

PAS staining and immunohistochemical analysis

Segmented mouse kidneys were fixed with 4% formalin, embedded in paraffin, and subsequently cut into 4-μm slices. PAS staining was carried out using a PAS kit (Jiancheng, Nanjing, China) according to the manufacturer's instructions. The proximal renal impairment score shows the extent of tubular necroptosis and tubular dilatation as follows: 0 = normal, 1 = 10%, 2 = 10%–25%, 3 = 26%–50%, 4 = 51%–75%, 5 = 76%–95%, and 6 = more than 96% [14]. Images were acquired with an Olympus BX51 microscope (Olympus, Center Valley, PA, USA). Quantification was performed by three investigators blinded to the experimental conditions.

For immunohistochemistry, kidney sections were treated with 0.01-M sodium citrate buffer (pH 6.0) by a microwave-based antigen retrieval technique for 20 min at 95 °C and were then incubated for 10 min with 3% H_2O_2 to block endogenous peroxidase activity. Samples were then incubated with rabbit anti-TNF-α, anti-F4/80, anti-Kim-1, and mouse anti-SFN antibodies for 24 h at 4 °C and with secondary antibodies for 30 min at 37 °C. After staining with DAB, slides were visualized under a microscope (Leica, Bensheim, Germany) [31, 32]. Quantification was performed by three investigators blinded to the experimental conditions.

Immunofluorescence

HK2 cells were cultured in eight-chamber glass slides, fixed with acetone, and incubated overnight with antibodies specific for Kim-1, p-MLKL, RIPK3, and SFN. Cells were washed with PBS and incubated with goat anti-rabbit and goat anti-mouse IgG-rhodamine (BiossBiotechnology, Beijing, China) for 2 h at room temperature. Cells were counterstained with DAPI and visualized using fluorescence microscopy (Leica, Bensheim, Germany), and semiquantitative analysis of IF images was conducted using IPWIN software as previously described [33].

Renal function detection

Blood was collected from mice after anesthesia. Serum was separated by centrifugation at 3000 r/min for 15 min at 4 °C and used to measure Cr and BUN using assay kits as previously described [34].

Coimmunoprecipitation

HK2 cells were washed three times with precooled PBS solution and lysed in NP-40 buffer. Samples were precipitated with the indicated antibodies (1 μg) and protein A/G-agarose beads (Santa Cruz, CA, USA) by incubation at 4 °C overnight. Beads were washed three times with 1 mL of NP-40 buffer, and bound proteins were then removed by boiling in SDS buffer and resolved on 4%–20% SDS–polyacrylamide gels for Western blot analysis.

Statistical analysis

The data acquired from this study are presented as the mean ± SEM of 3–4 independent in vitro experiments or 6–8 mice for in vivo studies. Statistical analyses were performed using a two-tailed unpaired *t* test or one-way ANOVA followed by the Newman–Keuls post hoc test (Prism 5.0; GraphPad Software, San Diego, CA). Differences were considered statistically significant at $P < 0.05$.

RESULTS

Upregulated SFN expression in AKI

To study changes in protein expression in AKI, proteomic analysis was performed by the iTRAQ method. As shown in Fig. 1a, SFN

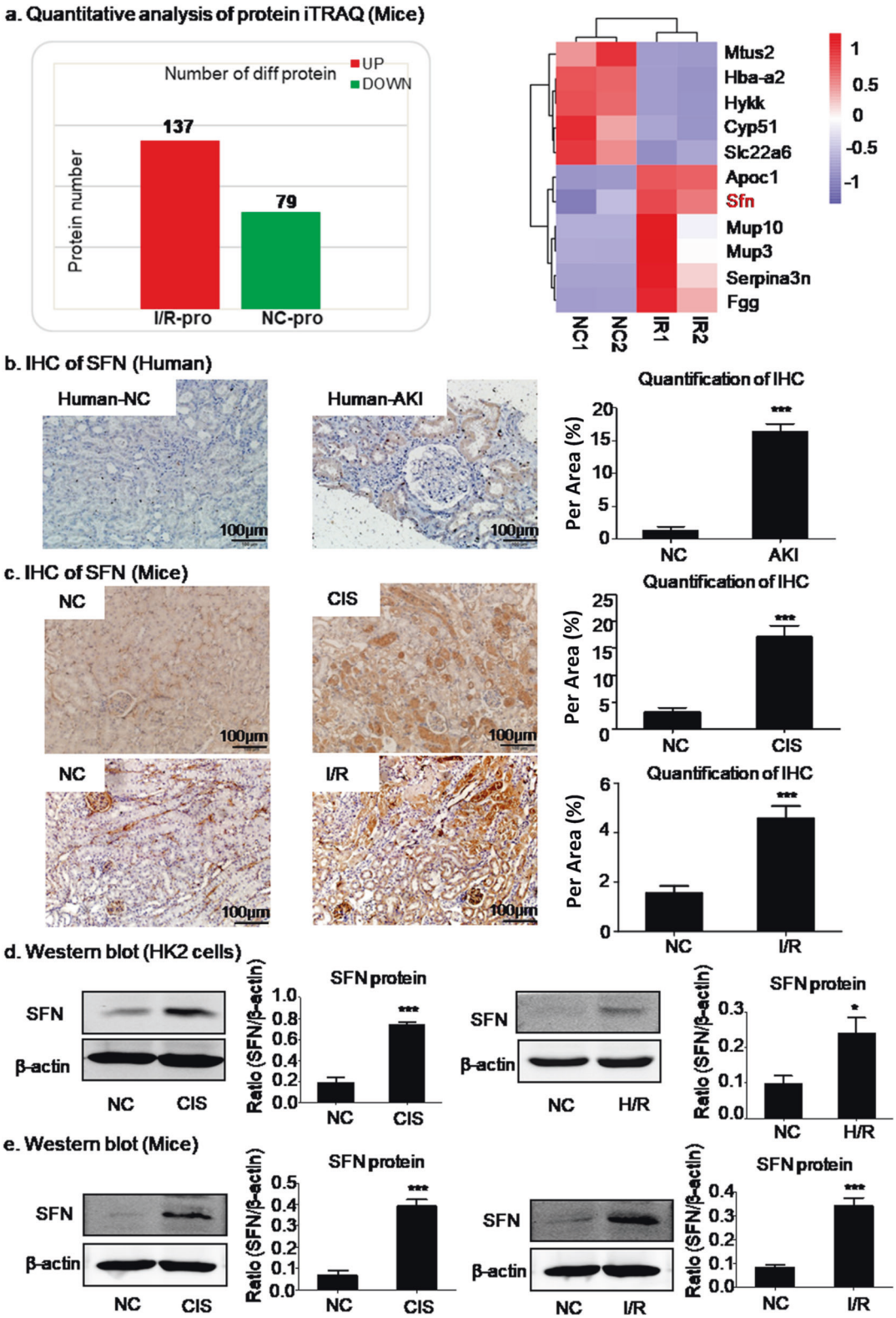

Fig. 1 Expression of SNF protein in AKI. a Quantitative protein analysis by the iTRAQ method in HK2 cells. SFN was highly expressed in I/R mice. **b**, **c** Immunohistochemical assay of SFN in AKI patients and mice. SFN was highly expressed in AKI patients and mice. Scale bars = 100 μm. **d** Western blot analysis of SFN in HK2 cells. Treatment with cisplatin- or H/R-induced upregulation of SFN. **e** Western blot analysis of SFN in mice with cisplatin- or I/R-induced AKI. Treatment with cisplatin- or I/R-induced upregulation of SFN. In vivo data are presented as the mean ± SEM of six mice, and in vitro data are presented as the mean ± SEM of 3–4 independent experiments (these numbers also apply to human samples). $^{*}P < 0.05$, $^{***}P < 0.001$ versus the normal group.

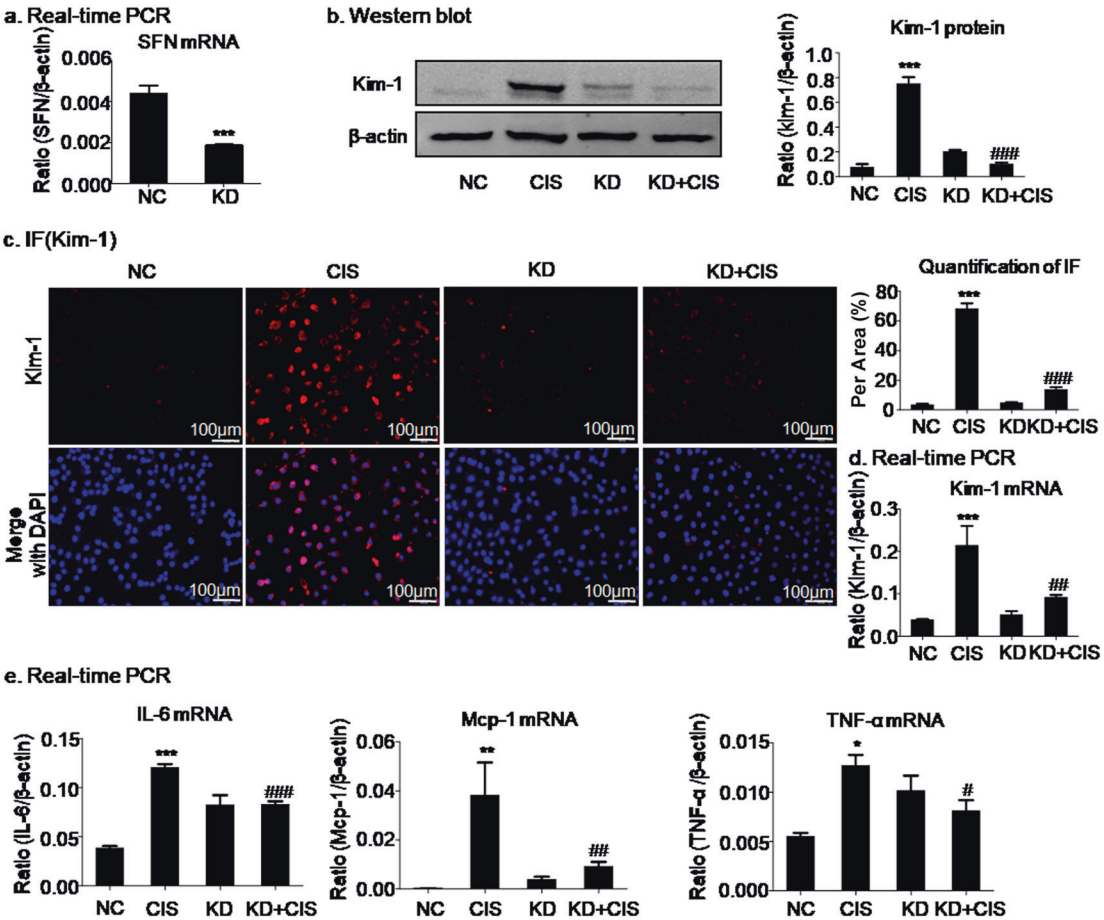

Fig. 2 SFN knockdown attenuated cisplatin-induced injury in HK2 cells. a Knockdown of SFN in HK2 cells by SFN siRNA. **b–d** Western blot, immunofluorescence, and real-time PCR analyses of Kim-1 in HK2 cells. Knockdown of SFN significantly decreased the protein and mRNA levels of Kim-1. Scale bars = 100 μm. **e** Real-time PCR analysis of inflammatory indexes. Knockdown of SFN reduced the mRNA levels of inflammatory cytokines, including IL-6, Mcp-1, and TNF-α, in HK2 cells treated with cisplatin. The data are presented as the mean ± SEM of 3–4 independent experiments in vitro. $^{*}P < 0.05$, $^{**}P < 0.01$, $^{***}P < 0.001$ versus the normal group; $^{\#}P < 0.05$, $^{\#\#}P < 0.01$, $^{\#\#\#}P < 0.001$ versus the cisplatin-treated group.

was expressed at a significantly higher level in I/R mice than were the other differentially expressed proteins. The same results were obtained in AKI patients and verified by immunohistochemistry in mice with cisplatin- or I/R-induced AKI (Fig. 1b, c). Western blot analysis further confirmed that SFN expression was upregulated in HK2 cells treated with cisplatin or subjected to H/R (Fig. 1d). In addition, the same conclusion was obtained in mice with cisplatin- or I/R-induced AKI through Western blot analysis (Fig. 1e).

SFN knockdown attenuated cisplatin- or H/R-induced injury in HK2 cells

SFN is highly expressed in multiple types of AKI, but its function is not fully understood. To assess the role of SFN, it was knocked down by transfection of HK2 cells with SFN siRNA (Fig. 2a). The real-time PCR, Western blot, and immunofluorescence results indicated that silencing SFN significantly reduced the mRNA and protein levels of the kidney injury marker Kim-1 in cisplatin-treated HK2 cells compared with empty vector control cells (Fig. 2b, c, d). Furthermore, silencing SFN suppressed the cisplatin-induced inflammatory response (IL-6, Mcp-1, and TNF-α levels) in cisplatin-treated HK2 cells (Fig. 2e).

We also established a model of H/R-induced damage in HK2 cells. SFN in HK2 cells was silenced by SFN siRNA (Fig. 3a). Consistent with the above results, the results of Western blotting and quantitative analysis showed that H/R induced the expression of Kim-1, but SFN knockdown reduced Kim-1 expression nearly to baseline levels (Fig. 3b). The suppressive effect of SFN knockdown on Kim-1 was further confirmed by immunofluorescence and real-time PCR in H/R-treated HK2 cells (Fig. 3c, d). We also measured the effect of SFN knockdown on the H/R-induced inflammatory response in HK2 cells, and the real-time PCR results showed that SFN knockdown significantly suppressed the inflammatory response in H/R-induced HK2 cells (Fig. 3e).

SFN knockdown significantly alleviated necroptosis in cisplatin- or H/R-treated HK2 cells

To elucidate the mechanism by which SFN promotes cell injury, we investigated whether necroptosis is involved. We then determined the effect of SFN knockdown on necroptosis by using Western blot and immunofluorescence analyses. The key signaling modulators in necroptosis, RIPK1, RIPK3, and p-MLKL were evaluated [33, 34]. Cisplatin increased the levels of all three proteins, whereas SFN knockdown notably inhibited the activation of the RIPK1/RIPK3/p-MLKL axis (Fig. 4a, b). To further confirm the inhibitory effect of SFN knockdown, we established another in vitro cell damage model of H/R-mediated necroptosis. Consistent with the above results, the results in this model also indicated that SFN knockdown significantly suppressed H/R-induced activation of the RIPK1/RIPK3/p-MLKL axis (Fig. 4c, d).

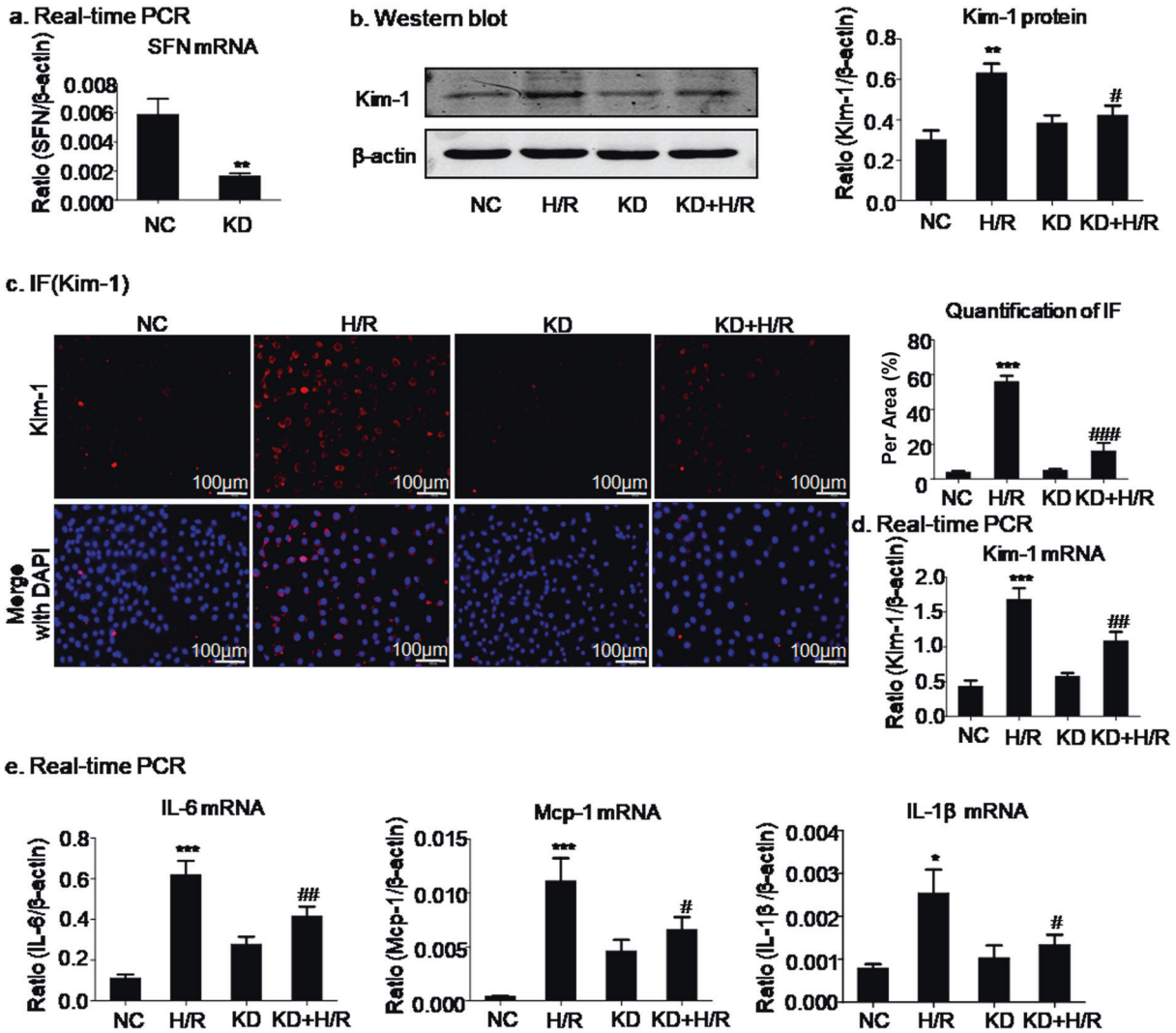

Fig. 3 SFN knockdown attenuated hypoxia/reoxygenation-induced injury in HK2 cells. a Knockdown of SFN in HK2 cells by SFN siRNA. **b–d** Western blot, immunofluorescence, and real-time PCR analyses of Kim-1 in HK2 cells. Knockdown of SFN significantly decreased the protein and mRNA levels of Kim-1. Scale bars = 100 μm. **e** Real-time PCR analysis of inflammatory indexes. Knockdown of SFN reduced the mRNA levels of inflammatory cytokines, including IL-6, Mcp-1, and IL-1β, in HK2 cells subjected to hypoxia/reoxygenation. The data are presented as the mean ± SEM of 3–4 independent experiments in vitro. $^{*}P < 0.05$, $^{**}P < 0.01$, $^{***}P < 0.001$ versus the normal group; $^{\#}P < 0.05$, $^{\#\#}P < 0.01$, $^{\#\#\#}P < 0.001$ versus the H/R-treated group.

SFN knockdown protected against cisplatin-induced kidney injury in the AKI mouse model

To validate SFN as a potential therapeutic target in the AKI mouse model, we injected mice with lentivirus-mediated SFN knockdown with cisplatin. Knockdown of SFN in vivo was demonstrated by Western blot analysis (Fig. 5a). The results of Western blot analysis and the quantitative data showed that SFN knockdown significantly suppressed cisplatin-induced SFN expression (Fig. 5b). Moreover, SFN knockdown improved renal function, as supported by assays of the serological indicators serum Cr and BUN (Fig. 5c, d).

The morphological characteristics of kidney tubular epithelial cells were investigated by PAS staining. Light microscopy revealed that the severe features of acute renal tubular epithelial cell necroptosis in AKI mice, including cell swelling and sloughing and dilation of renal tubules, were significantly alleviated by SFN knockdown (Fig. 5e). Consistent with these results, the immunohistochemical and real-time PCR results also showed that SFN knockdown suppressed the cisplatin-induced increases in Kim-1 protein and mRNA levels (Fig. 5f, g).

SFN knockdown attenuated renal injury in vivo by targeting necroptosis

We previously observed that SFN promoted cisplatin-induced renal injury associated with the activation of necroptosis in HK2 cells. Furthermore, we confirmed this finding in a mouse model of cisplatin-induced AKI. As a result, we found that knockdown of SFN in vivo reduced the levels of RIPK1 and RIPK3, which could result in decreased necroptosis and thus attenuate AKI (Fig. 6a). In addition, the results of immunofluorescence and quantitative analyses showed that cisplatin significantly activated p-MLKL, which was inhibited by SFN knockdown (Fig. 6e). In addition, evaluation of the expression of inflammatory factors such as TNF-α, IL-1β, and IL-6 showed that knockdown of SFN could have an anti-inflammatory effect, which was verified by real-time PCR analysis (Fig. 6b). We also performed immunohistochemical analysis of TNF-α and F4/80. Through analysis of these data, it was found that knockdown of SFN reduced macrophage infiltration and the inflammatory response, showing the same result indicated by real-time PCR (Fig. 6c, d).

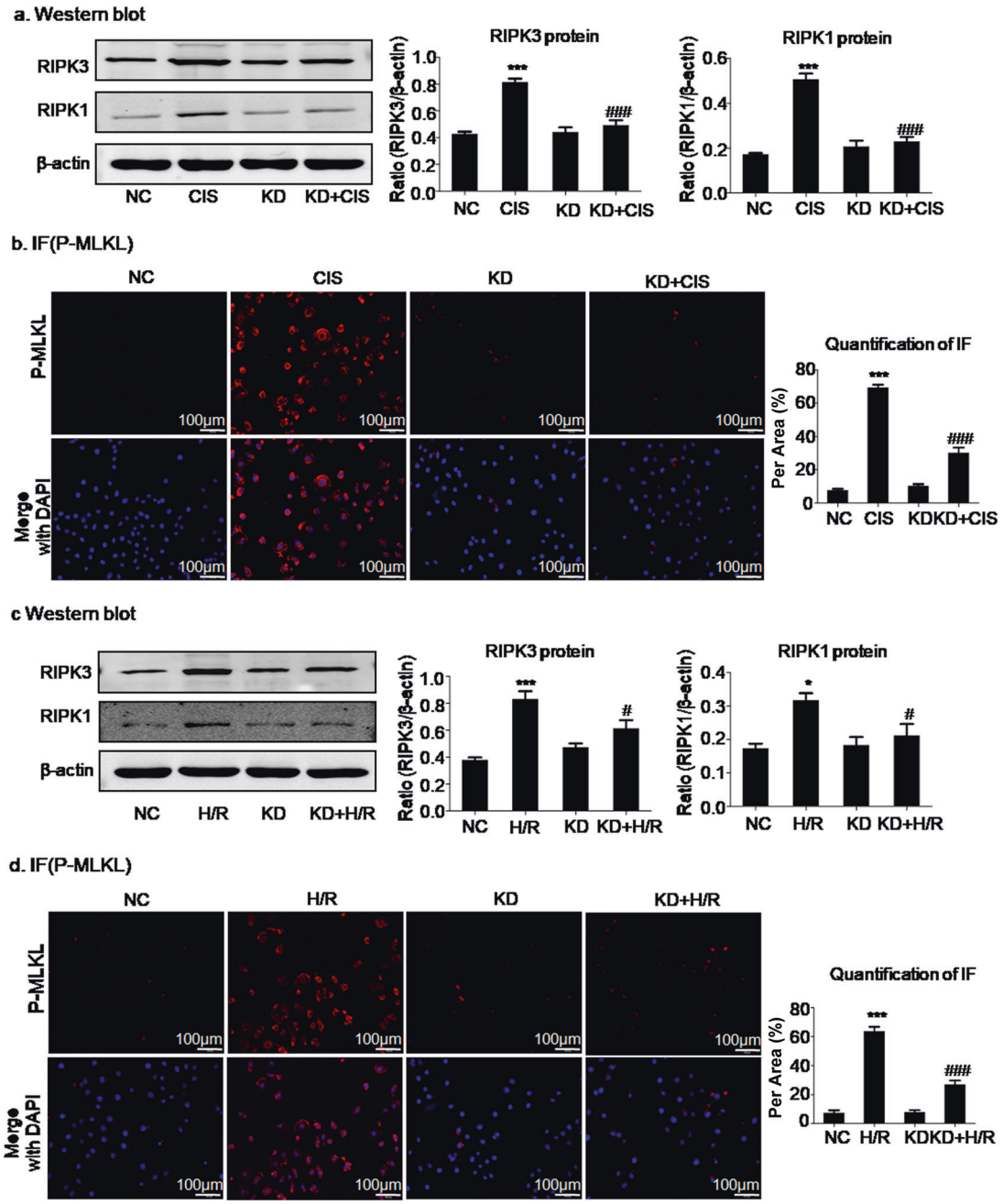

Fig. 4 SFN knockdown significantly attenuated programmed cell death in cisplatin- and H/R-treated HK2 cells. a, **b** Western blot and immunofluorescence analyses of programmed cell death-related molecules in HK2 cells treated with cisplatin. Knockdown of SFN significantly decreased the levels of necroptosis-related markers, including RIPK1, RIPK3, and p-MLKL. **c**, **d** Western blot and immunofluorescence analyses of programmed cell death-related molecules in HK2 cells treated with H/R. Knockdown of SFN significantly decreased RIPK1, RIPK3, and p-MLKL levels. Scale bars = 100 μm. The data are presented as the mean ± SEM of 3–4 independent experiments in vitro. $^{*}P < 0.05$, $^{***}P < 0.001$ versus the normal group; $^{\#}P < 0.05$, $^{\#\#\#}P < 0.001$ versus the cisplatin- or H/R-treated group.

SFN promoted cisplatin-induced cell injury by interacting with RIPK3

To determine the mechanism by which SFN mediates necroptosis, lysates of cisplatin- or H/R-treated HK2 cells were extracted for Co-IP of SFN and key necroptotic signaling modulators. The Co-IP results confirmed that SFN bound directly to RIPK3 but not RIPK1 (Fig. 7a). In addition, to further validate the relationship between SNF and RIPK3, colocalization of SFN and RIPK3 was assessed by immunofluorescence. The results of immunofluorescence and quantitative analyses also showed colocalization of RIPK3 and SFN (Fig. 7b, c).

Knockout of RIPK3 prevented SFN-mediated cisplatin-induced cell injury

To further explore the interaction of SFN and RIPK3, MTECs with RIPK3 knockout were established (Fig. 8a). Moreover, MTECs with SFN OE were established to further verify the interaction of SFN with RIPK3. Western blot and quantitative analyses showed that OE of SFN enhanced the Kim-1 protein level in MTECs with cisplatin-induced injury and that this increase was suppressed by RIPK3 knockout (Fig. 8a), and the immunofluorescence results were consistent with the above conclusion (Fig. 8b). These results

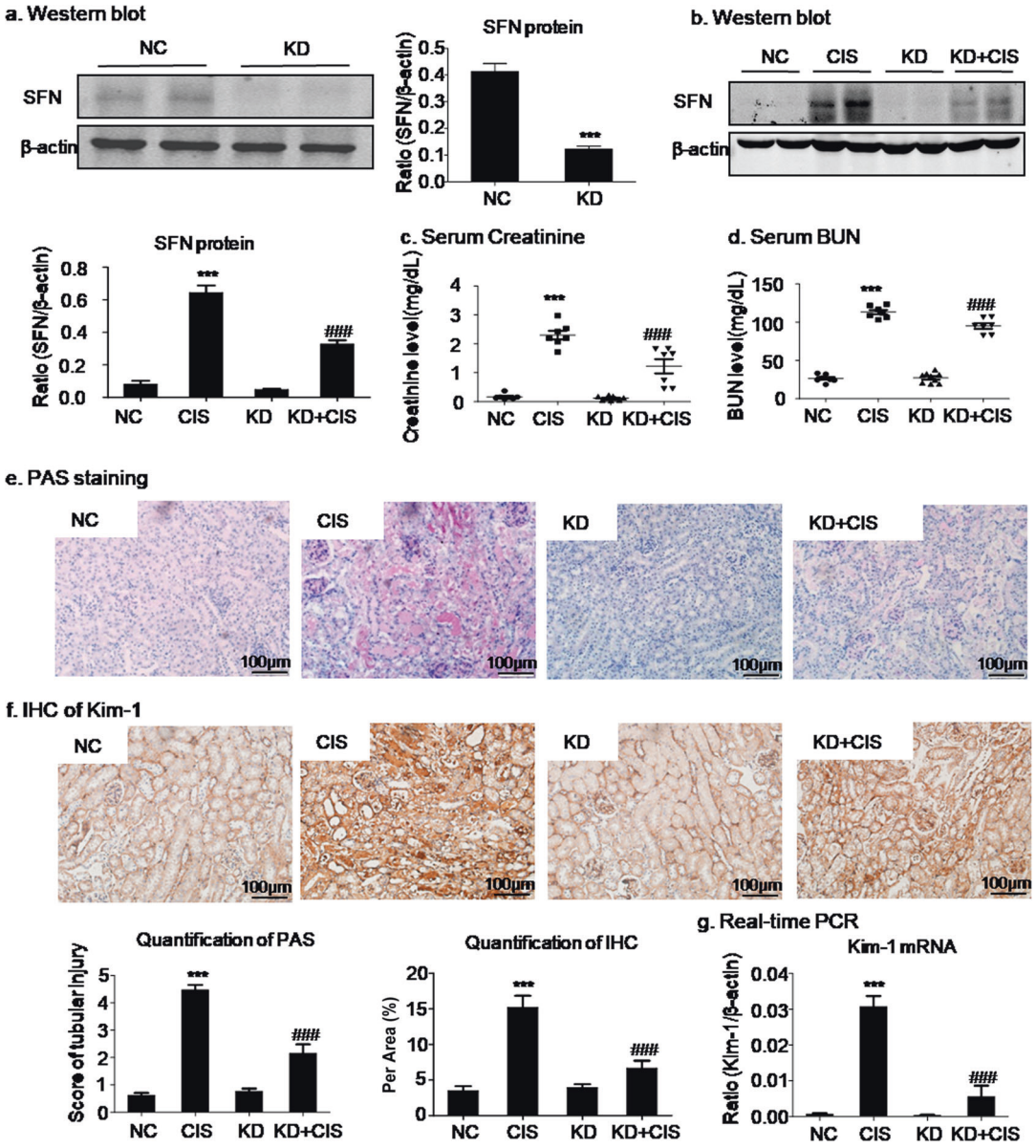

Fig. 5 SFN knockdown protected against cisplatin-induced kidney injury in vivo. a, **b** Western blot analysis of SFN knockdown in mice. **c**, **d** Renal function. The serum creatinine and BUN levels showed that SFN knockdown suppressed the decline in renal function caused by cisplatin. **e** Periodic acid-Schiff (PAS) staining. SFN knockdown prevented cisplatin-induced renal injury in vivo. Scale bars = 100 μm. **f**, **g** Immunohistochemical and real-time PCR analyses of Kim-1. SFN knockdown reduced the protein and mRNA levels of Kim-1 in mice with cisplatin-induced nephropathy. Scale bars = 100 μm. The data are presented as the mean ± SEM of six mice in vivo. $^{***}P < 0.001$ versus the normal group; $^{\#\#\#}P < 0.001$ versus the cisplatin group.

suggested that SFN promoted cisplatin-induced cell injury by interacting with RIPK3.

DISCUSSION

In the current study, we found that SFN promoted cisplatin- and H/R-induced renal injury both in vivo and in vitro. Our findings showed that SFN accelerated AKI by interacting with RIPK3, which was possibly correlated with its regulatory role in renal programmed cell death and inflammation.

It was verified that the protein expression of SFN was upregulated after kidney injury [16]; however, the function of SFN in AKI remains to be determined. We found that cisplatin and H/R significantly upregulated SFN in tubular epithelial cells and injured kidneys. To further explore its functional role, we knocked down SFN in cisplatin- and H/R-treated tubular epithelial cells of mouse and human origin and discovered that the expression of Kim-1, a key index of kidney injury, was significantly reduced. This finding was consistent with the results of our in vivo study showing that lentivirus-mediated knockdown of SFN attenuated the deterioration of renal function and tubular damage.

The mechanisms by which SFN knockdown prevented cisplatin- and H/R-induced cell injury were then evaluated. SFN regulates cell death in immune and tumor cells [19, 21]. Our previous study showed that cisplatin and H/R activated necroptosis in tubular epithelial cells [13, 35–37]. Programmed necroptosis is mediated by RIPK1/RIPK3/MLKL activation under pathologic conditions [38]. When injury signals are transduced to RIPK1, a key molecule in

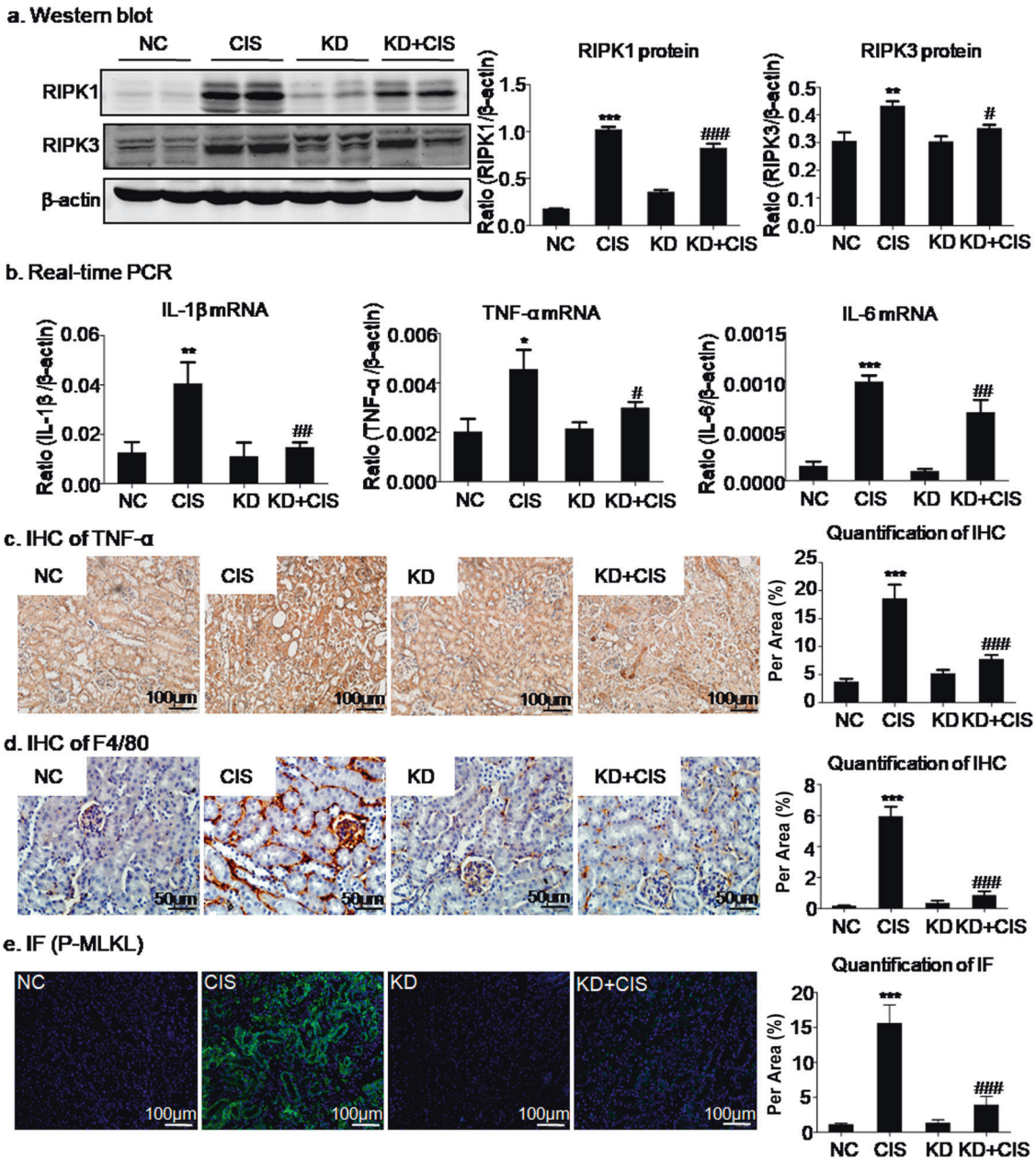

Fig. 6 Knockdown of SFN attenuated renal injury in vivo. a Western blot analysis of programmed cell death-related molecules in vivo. Knockdown of SFN significantly downregulated the expression of RIPK1 and RIPK3. **b** Real-time PCR analysis of inflammatory indexes. Knockdown of SFN reduced the mRNA levels of inflammatory cytokines, including IL-6, IL-1β, and TNF-α, in cisplatin-treated mice. **c** Immunohistochemical analysis of TNF-α. Knockdown of SFN reduced TNF-α expression in cisplatin-treated mice. Scale bars = 100 μm. **d** Immunohistochemical analysis of F4/80. Knockdown of SFN significantly inhibited macrophage infiltration. Scale bars = 50 μm. **e** Immunofluorescence analysis of p-MLKL showed that knockdown of SFN in vivo significantly reduced cisplatin-induced membrane translocation of p-MLKL. Scale bars = 100 μm. The data are presented as the mean ± SEM of six mice in vivo. $^{*}P < 0.05$, $^{**}P < 0.01$, $^{***}P < 0.001$ versus normal mice. $^{\#}P < 0.05$, $^{\#\#\#}P < 0.001$ versus vector control mice.

necroptosis initiation, RIPK1 recruits and binds with RIPK3 and then promotes translocation of p-MLKL to the plasma membrane, leading to disruption of this membrane [39]. Pharmacological inhibition of RIPK1 and knockdown of the RIPK3 and MLKL proteins prevents kidney injury caused by cisplatin [14, 23, 36]. These findings indicate a critical role for RIPK-mediated necroptosis in cisplatin-induced AKI. Necroptosis is a regulated process involving cell lysis leading to cell death and is controlled by specific kinases. It is characterized by swelling of cells and organelles, which is followed by permeability of the cell membrane. This is a typical pattern of cell death due to accidental injury, and it is also a form of programmed cell death [40, 41]. RIPK3 can trigger the necroptosis pathway independent of RIPK1, and MLKL is considered to be the main and possibly the only target involved in RIPK3-mediated cell death. RIPK1 and/or RIPK3 regulate the production of proinflammatory cytokines and promote renal inflammation [42]. Our previous study verified that inhibition of necroptosis can reduce inflammation and protect against kidney injury [26]. Our Co-IP and immunofluorescence data provided evidence of the

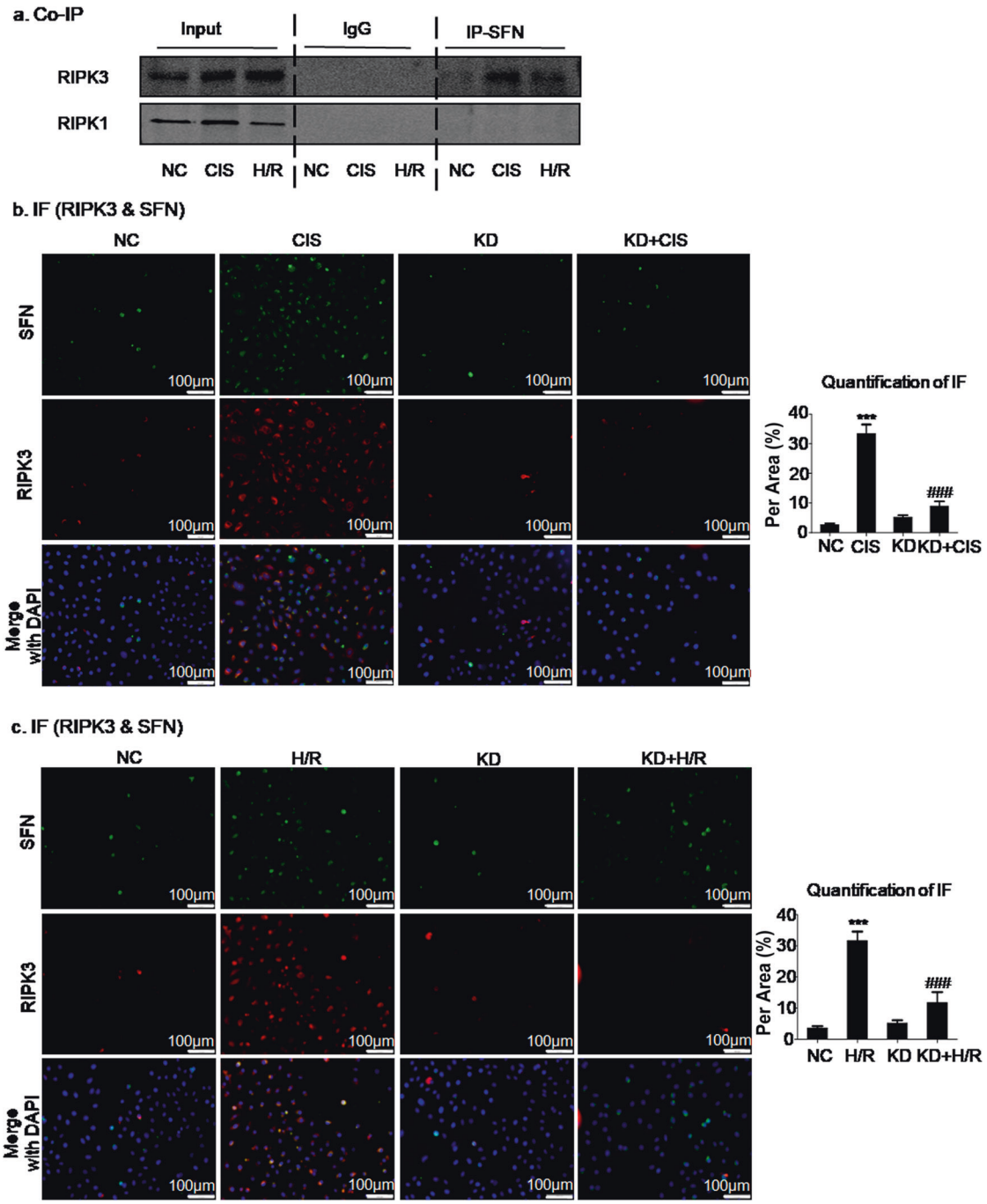

Fig. 7 SFN interacts with RIPK3 in cisplatin- and H/R-induced HK2 cells. a Co-IP of SFN and key modulators of necroptotic signaling. **b**, **c** Immunofluorescence analysis confirmed the colocalization of SFN and RIPK3 in cisplatin- and H/R-induced cell injury models. Scale bars = 100 μm. The data are presented as the mean ± SEM of 3–4 independent experiments in vitro. $^{***}P < 0.001$, versus the normal group; $^{###}P < 0.001$ versus the cisplatin-treated or H/R-treated group.

potential interaction of SFN with RIPK3, and we found that loss of SFN prevented but OE of SFN promoted cisplatin-activated necroptotic signaling. This result indicates that SFN may play an important role in mediating cell necroptosis and consequent necroinflammation. More importantly, we overexpressed SFN in RIPK3-KO cell lines to further confirm the mechanisms by which SFN promotes cell injury; our results showed that when RIPK3 was lost, SFN failed to enhance renal injury, and these data collectively indicated that SFN promoted cell injury possibly by interacting with RIPK3.

Emerging evidence shows that necroptosis triggers a severe inflammatory response by destroying cell membranes, facilitating the release of endogenous proinflammatory molecules [43]. It has been confirmed that 14-3-3 proteins affect inflammation at the genetic, molecular, and cellular levels in diverse inflammatory diseases [44, 45]; in addition, the anti-necroptotic effects of SFN knockdown may contribute to attenuation of renal inflammation. In the current study, we found that SFN knockdown attenuated cisplatin- and H/R-induced inflammatory responses, which was verified by the decreased production of proinflammatory

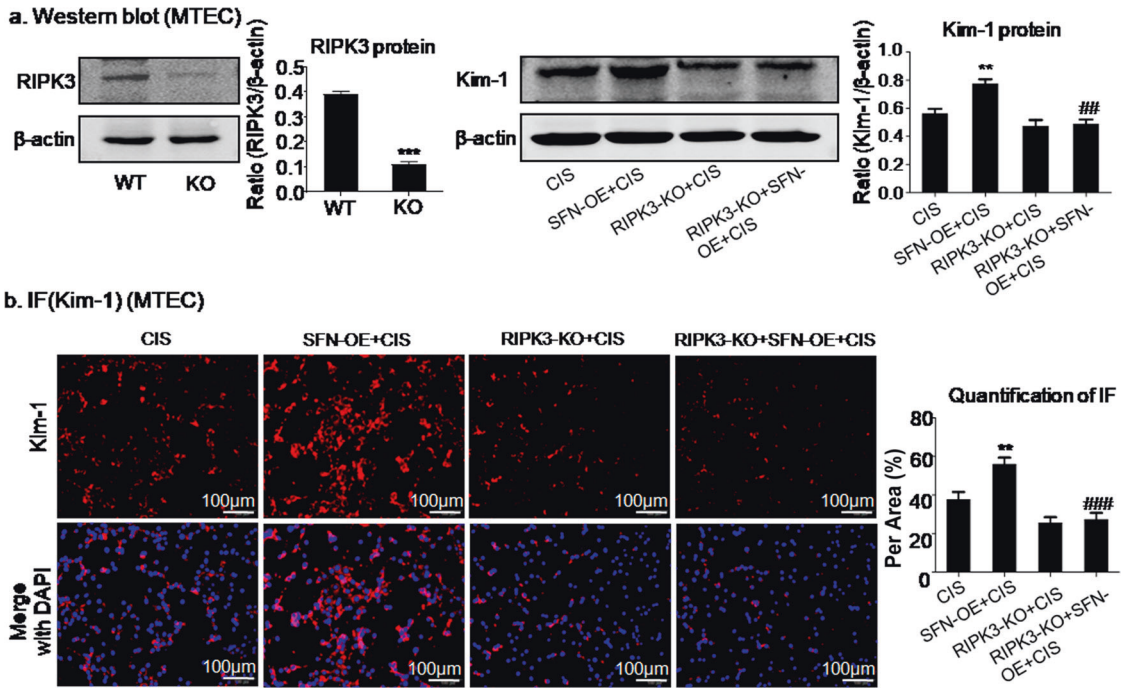

Fig. 8 SFN promoted cisplatin-induced HK2 cell injury via interaction with RIPK3. a Western blot analysis of RIPK3 and Kim-1. **b** Immunofluorescence analysis of the Kim-1 protein. Overexpression of SFN promoted the protein and mRNA expression of Kim-1 in cisplatin-treated MTECs, which was inhibited by RIPK3 knockout. Scale bars = 100 μm. The data are presented as the mean ± SEM of 3–4 independent experiments in vitro. $^{**}P < 0.01$, versus the cisplatin group; $^{\#\#}P < 0.01$, $^{\#\#\#}P < 0.001$, versus the cisplatin-treated SFN OE group.

cytokines, including IL-6, Mcp-1, and TNF-α. In addition, the regulatory role of SFN knockdown on macrophage infiltration may also be responsible for the anti-inflammatory effect of SFN on AKI. These findings suggest that SFN knockdown suppresses RIPK-mediated necroptosis, which alleviates cisplatin- and H/R-induced kidney injury and inflammation.

Finally, by lentivirus-mediated shRNA knockdown of SFN via tail vein injection, we tested whether SFN is a potential therapeutic target in a mouse model of cisplatin-induced nephropathy. Our results showed that SFN inhibition prevented deterioration of renal function while relieving kidney damage and inflammation. Consistent with this result, loss of SFN in the kidney reduced cisplatin-induced cell necroptosis and inflammation.

In conclusion, we showed that cisplatin- and H/R-induced kidney injury, programmed cell death, and inflammation are mediated via SFN-related mechanisms. In vivo, SFN knockdown effectively attenuated cisplatin-induced kidney damage, programmed cell death, and inflammation, indicating that SFN might be a therapeutic target in AKI.

ACKNOWLEDGEMENTS

We thank the Center for Scientific Research of Anhui Medical University for valuable help in our experiment. This work was supported by the National Natural Science Foundation of China (No. 81970584). Promotion plan of basic and clinical cooperative research in Anhui Medical University (No. 2019xkjT014; No. 2020xkjT016).

AUTHOR CONTRIBUTIONS

FW, JNW, and XYH performed the cell experiment, analyzed the data, and wrote the manuscript. XMM and JJ designed, supervised, and wrote the manuscript. CL, WJN, YTC, XZ, and YRY provided a series of experimental instructions and help. XGS, YH, XYF, and YHD performed the animal experiments. FZ, TX, HMZ, MML, and JL contributed new reagents or analytic tools.

ADDITIONAL INFORMATION

Supplementary information The online version contains supplementary material available at https://doi.org/10.1038/s41401-021-00649-w.

Competing interests: The authors declare no competing interests.

REFERENCES

1. Gao L, Zhong X, Jin J, Li J, Meng XM. Potential targeted therapy and diagnosis based on novel insight into growth factors, receptors, and downstream effectors in acute kidney injury and acute kidney injury-chronic kidney disease progression. Signal Transduct Target Ther. 2020;5:9.
2. Fortrie G, de Geus HRH, Betjes MGH. The aftermath of acute kidney injury: a narrative review of long-term mortality and renal function. Crit Care. 2019;23:24.
3. Tarvasmaki T, Haapio M, Mebazaa A, Sionis A, Silva-Cardoso J, Tolppanen H, et al. Acute kidney injury in cardiogenic shock: definitions, incidence, haemodynamic alterations, and mortality. Eur J Heart Fail. 2018;20:572–81.
4. Gonsalez SR, Cortes AL, Silva RCD, Lowe J, Prieto MC, Silva Lara LD. Acute kidney injury overview: from basic findings to new prevention and therapy strategies. Pharmacol Ther. 2019;200:1–12.
5. Liu KD, Yang J, Tan TC, Glidden DV, Zheng S, Pravoverov L, et al. Risk factors for recurrent acute kidney injury in a large population-based cohort. Am J Kidney Dis. 2019;73:163–73.
6. McCoy IE, Chertow GM. AKI-A relevant safety end point? Am J Kidney Dis. 2020;75:508–12.
7. Brandenburger T, Salgado Somoza A, Devaux Y, Lorenzen JM. Noncoding RNAs in acute kidney injury. Kidney Int. 2018;94:870–81.
8. Peerapornratana S, Manrique-Caballero CL, Gomez H, Kellum JA. Acute kidney injury from sepsis: current concepts, epidemiology, pathophysiology, prevention and treatment. Kidney Int. 2019;96:1083–99.
9. Maheshwari K, Nathanson BH, Munson SH, Khangulov V, Stevens M, Badani H, et al. The relationship between ICU hypotension and in-hospital mortality and morbidity in septic patients. Intensive Care Med. 2018;44:857–67.
10. Sun J, Zhang J, Tian J, Virzi GM, Digvijay K, Cueto L, et al. Mitochondria in sepsis-induced AKI. J Am Soc Nephrol. 2019;30:1151–61.
11. Noel S. Orai1: CRACing the Th17 response in AKI. J Clin Invest. 2019;129:4583–6.

12. Mishima E, Sato E, Ito J, Yamada KI, Suzuki C, Oikawa Y, et al. Drugs repurposed as antiferroptosis agents suppress organ damage, including AKI, by functioning as lipid peroxyl radical scavengers. J Am Soc Nephrol. 2020;31:280–96.
13. Gao L, Wu WF, Dong L, Ren GL, Li HD, Yang Q, et al. Protocatechuic aldehyde attenuates cisplatin-induced acute kidney injury by suppressing nox-mediated oxidative stress and renal inflammation. Front Pharmacol. 2016;7:479.
14. Wang JN, Liu MM, Wang F, Wei B, Yang Q, Cai YT, et al. RIPK1 inhibitor Cpd-71 attenuates renal dysfunction in cisplatin-treated mice via attenuating necroptosis, inflammation and oxidative stress. Clin Sci. 2019;133:1609–27.
15. Rizou M, Frangou EA, Marineli F, Prakoura N, Zoidakis J, Gakiopoulou H, et al. The family of 14-3-3 proteins and specifically 14-3-3sigma are up-regulated during the development of renal pathologies. J Cell Mol Med. 2018;22:4139–49.
16. Suarez-Bonnet A, Lara-Garcia A, Stoll AL, Carvalho S, Priestnall SL. 14-3-3sigma protein expression in canine renal cell carcinomas. Vet Pathol. 2018;55:233–40.
17. Darling DL, Yingling J, Wynshaw-Boris A. Role of 14-3-3 proteins in eukaryotic signaling and development. Curr Top Dev Biol. 2005;68:281–315.
18. Mhawech P. 14-3-3 proteins–an update. Cell Res. 2005;15:228–36.
19. Munier CC, Ottmann C, Perry MWD. 14-3-3 modulation of the inflammatory response. Pharmacol Res. 2021;163:105236.
20. Robin F, Angenard G, Cano L, Courtin-Tanguy L, Gaignard E, Khene ZE, et al. Molecular profiling of stroma highlights stratifin as a novel biomarker of poor prognosis in pancreatic ductal adenocarcinoma. Br J Cancer. 2020;123:72–80.
21. Sime W, Niu Q, Abassi Y, Masoumi KC, Zarrizi R, Kohler JB, et al. BAP1 induces cell death via interaction with 14-3-3 in neuroblastoma. Cell Death Dis. 2018;9:458.
22. Sirivatanauksorn V, Dumronggittigule W, Dulnee B, Srisawat C, Sirivatanauksorn Y, Pongpaibul A, et al. Role of stratifin (14-3-3 sigma) in adenocarcinoma of gallbladder: a novel prognostic biomarker. Surg Oncol. 2020;32:57–62.
23. Xu Y, Ma H, Shao J, Wu J, Zhou L, Zhang Z, et al. A role for tubular necroptosis in cisplatin-induced AKI. J Am Soc Nephrol. 2015;26:2647–58.
24. Liu W, Chen B, Wang Y, Meng C, Huang H, Huang XR, et al. RGMb protects against acute kidney injury by inhibiting tubular cell necroptosis via an MLKL-dependent mechanism. Proc Natl Acad Sci U S A. 2018;115:E1475–84.
25. Zhu H, Sun A. Programmed necrosis in heart disease: molecular mechanisms and clinical implications. J Mol Cell Cardiol. 2018;116:125–34.
26. Yang Q, Ren GL, Wei B, Jin J, Huang XR, Shao W, et al. Conditional knockout of TGF-betaRII /Smad2 signals protects against acute renal injury by alleviating cell necroptosis, apoptosis and inflammation. Theranostics. 2019;9:8277–93.
27. Abais JM, Xia M, Li G, Chen Y, Conley SM, Gehr TW, et al. Nod-like receptor protein 3 (NLRP3) inflammasome activation and podocyte injury via thioredoxin-interacting protein (TXNIP) during hyperhomocysteinemia. J Biol Chem. 2014;289:27159–68.
28. Pang P, Jin X, Proctor BM, Farley M, Roy N, Chin MS, et al. RGS4 inhibits angiotensin II signaling and macrophage localization during renal reperfusion injury independent of vasospasm. Kidney Int. 2015;87:771–83.
29. Fettweis G, Di Valentin E, L'Homme L, Lassence C, Dequiedt F, Fillet M, et al. RIP3 antagonizes a TSC2-mediated pro-survival pathway in glioblastoma cell death. Biochim Biophys Acta Mol Cell Res. 2017;1864:113–24.
30. Liu Y, Liu T, Lei T, Zhang D, Du S, Girani L, et al. RIP1/RIP3-regulated necroptosis as a target for multifaceted disease therapy (Review). Int J Mol Med. 2019;44:771–86.
31. Meng XM, Huang XR, Chung AC, Qin W, Shao X, Igarashi P, et al. Smad2 protects against TGF-beta/Smad3-mediated renal fibrosis. J Am Soc Nephrol. 2010;21:1477–87.
32. Wang S, Meng XM, Ng YY, Ma FY, Zhou S, Zhang Y, et al. TGF-beta/Smad3 signalling regulates the transition of bone marrow-derived macrophages into myofibroblasts during tissue fibrosis. Oncotarget. 2016;7:8809–22.
33. Deng XX, Li SS, Sun FY. Necrostatin-1 prevents necroptosis in brains after ischemic stroke via inhibition of RIPK1-mediated RIPK3/MLKL signaling. Aging Dis. 2019;10:807–17.
34. Zhang YY, Liu WN, Li YQ, Zhang XJ, Yang J, Luo XJ, et al. Ligustroflavone reduces necroptosis in rat brain after ischemic stroke through targeting RIPK1/RIPK3/MLKL pathway. Naunyn Schmiedebergs Arch Pharmacol. 2019;392:1085–95.
35. Meng XM, Ren GL, Gao L, Yang Q, Li HD, Wu WF, et al. NADPH oxidase 4 promotes cisplatin-induced acute kidney injury via ROS-mediated programmed cell death and inflammation. Lab Invest. 2018;98:63–78.
36. Meng XM, Li HD, Wu WF, Ming-Kuen Tang P, Ren GL, Gao L, et al. Wogonin protects against cisplatin-induced acute kidney injury by targeting RIPK1-mediated necroptosis. Lab Invest. 2018;98:79–94.
37. Wang JN, Yang Q, Yang C, Cai YT, Xing T, Gao L, et al. Smad3 promotes AKI sensitivity in diabetic mice via interaction with p53 and induction of NOX4-dependent ROS production. Redox Biol. 2020;32:101479.
38. Jing L, Song F, Liu Z, Li J, Wu B, Fu Z, et al. MLKL-PITPalpha signaling-mediated necroptosis contributes to cisplatin-triggered cell death in lung cancer A549 cells. Cancer Lett. 2018;414:136–46.
39. Deepa SS, Unnikrishnan A, Matyi S, Hadad N, Richardson A. Necroptosis increases with age and is reduced by dietary restriction. Aging Cell. 2018;17:e12770.
40. Tonnus W, Meyer C, Paliege A, Belavgeni A, von Massenhausen A, Bornstein SR, et al. The pathological features of regulated necrosis. J Pathol. 2019;247:697–707.
41. Wallach D, Kang TB, Dillon CP, Green DR. Programmed necrosis in inflammation: toward identification of the effector molecules. Science. 2016;352:aaf2154.
42. Newton K. RIPK1 and RIPK3: critical regulators of inflammation and cell death. Trends Cell Biol. 2015;25:347–53.
43. Huang Z, Zhou T, Sun X, Zheng Y, Cheng B, Li M, et al. Necroptosis in microglia contributes to neuroinflammation and retinal degeneration through TLR4 activation. Cell Death Differ. 2018;25:180–9.
44. Cascio S, Medsger TA Jr, Hawse WF, Watkins SC, Milcarek C, Moreland LW, et al. 14-3-3z sequesters cytosolic T-bet, upregulating IL-13 levels in TC2 and $CD8^{+}$ lymphocytes from patients with scleroderma. J Allergy Clin Immunol. 2018;142:109–19.e6.
45. Kilani RT, Maksymowych WP, Aitken A, Boire G, St-Pierre Y, Li Y, et al. Detection of high levels of 2 specific isoforms of 14-3-3 proteins in synovial fluid from patients with joint inflammation. J Rheumatol. 2007;34:1650–7.